6952 *Inorg. Chem.* **2009**, *48*, 6952–6959
DOI: 10.1021/ic900181c

Inorganic Chemistry
Article

Preparation of Nb-Substituted Titanates by a Novel Sol−Gel Assisted Solid State Reaction

Haiyan Song,[†] Anja O. Sjåstad,[†] Ørnulv B. Vistad,[‡] Tao Gao,[†] and Poul Norby*[,†]

[†]*Department of Chemistry and Centre for Materials Science and Nanotechnology, University of Oslo, P.O. Box 1033, Blindern, N-0315 Oslo, Norway, and* [‡]*SINTEF Materials and Chemistry, P.O. Box 124, Blindern, N-0314 Oslo, Norway*

Received January 28, 2009

Single-phase layered Nb-substituted titanates, $Na_2Ti_{3-x}Nb_xO_7$ ($x = 0-0.06$) and $Cs_{0.7}Ti_{1.8-x}Nb_xO_4$ ($x = 0-0.03$), were for the first time synthesized by a novel sol−gel assisted solid state reaction (SASSR) route. Conventional solid state reactions as well as sol−gel synthesis did not succeed in producing phase pure Nb-substituted titanates. In the SASSR synthesis route we combine the advantages of traditional sol−gel technique (i.e., homogeneous products formed at low temperatures) and solid state reaction (i.e., formation of stable, crystalline phases) for preparing single-phase niobium-substituted layered titanates. The obtained products were characterized by X-ray powder diffraction, scanning electron microscopy, inductively coupled plasma-atomic emission spectrometry, Raman spectroscopy, and thermogravimetric analysis. Results indicate that the Ti(IV) in the host layer of the samples could be partially replaced by Nb(V) without structural deterioration. After proton-exchange, more water molecules were intercalated into the interlayer of $H_{0.7}Ti_{1.8-x}Nb_xO_4 \cdot nH_2O$ with increasing niobium content, whereas the interlayer distance of $H_2Ti_{3-x}Nb_xO_7$ ($x = 0-0.06$) was unchanged.

1. Introduction

Layered materials as, for example, layered double hydroxides (LDH) and layered titanates and niobates have been reported to exfoliate into single layer nanosheets,[1−5] and production of ultrathin films based on exfoliated layers originating from titanates[4] and niobates[5] are reported. Among the layered titanates, exfoliation and film preparation of $Cs_{0.7}Ti_{1.825}\Lambda_{0.175}O_4$ (Λ = vacancy) with lepidocrocite (γ-FeOOH)-type layered structure,[6] has been extensively investigated.[7−13] Sodium tri-titanate ($Na_2Ti_3O_7$), crystallizing with a monoclinic symmetry and having a larger surface charge density, has also been successfully exfoliated by intercalation of methylamine and propylamine.[14]

Exfoliated nanosheets are characterized to have the same structural atomic arrangement and chemical composition as the parent phase. Our group has worked with delamination and restacking of LDH,[1,15] and a natural extension for us is to focus on the delamination and fabrication of substituted-titanate nanosheets and the subsequent production of functional oxide films, for example, transparent conductive oxides (TCO) films,[16,17] from exfoliated layers.

*To whom correspondence should be addressed. E-mail: poul.norby@kjemi.uio.no. Phone: +47-22855566. Fax: +47-22855565.

(1) Wu, Q.-L.; Olafsen, A.; Vistad, Ø. B.; Roots, J.; Norby, P. *J. Mater. Chem.* **2005**, *15*, 4695.
(2) Joensen, P.; Frindt, R. F.; Morrison, S. R. *Mater. Res. Bull.* **1986**, *21*, 457.
(3) Treacy, M. M. J.; Rice, S. B.; Jacobson, A. J.; Lewandowski, J. T. *Chem. Mater.* **1990**, *2*, 279.
(4) Abe, R.; Shinohara, K.; Tanaka, A.; Hara, M.; Kondo, J. N.; Domen, K. *Chem. Mater.* **1998**, *10*, 329.
(5) Keller, S. W.; Kim, H.-N.; Mallouk, T. E. *J. Am. Chem. Soc.* **1994**, *116*, 8817.
(6) Grey, I. E.; Li, C.; Madsen, I. C.; Watts, J. A. *J. Solid State Chem.* **1987**, *66*, 7.
(7) Sasaki, T.; Watanabe, M. *J. Am. Chem. Soc.* **1998**, *120*, 4682.
(8) Sasaki, T.; Watanabe, M.; Hashizume, H.; Yamada, H.; Nakazawa, H. *J. Am. Chem. Soc.* **1996**, *118*, 8329.
(9) Sasaki, T.; Nakano, S.; Yamauchi, S.; Watanabe, M. *Chem. Mater.* **1997**, *9*, 602.
(10) Sasaki, T.; Watanabe, M.; Hashizume, H.; Yamada, H.; Nakazawa, H. *Chem. Commun.* **1996**, *2*, 229.
(11) Sasaki, T.; Ebina, Y.; Tanaka, T.; Harada, M.; Watanabe, M.; Decher, G. *Chem. Mater.* **2001**, *13*, 4661.
(12) Sasaki, T.; Ebina, Y.; Fukuda, K.; Tanaka, T.; Harada, M.; Watanabe, M. *Chem. Mater.* **2002**, *14*, 3524.
(13) Wang, Z.-S.; Sasaki, T.; Muramatsu, M.; Ebina, Y.; Tanaka, T.; Wang, L.-Z.; Watanabe, M. *Chem. Mater.* **2003**, *15*, 807.
(14) Miyamoto, N.; Kuroda, K.; Ogawa, M. *J . Mater . Chem.* **2004**, *14*, 165.
(15) (a) Wu, Q.-L.; Sjåstad, A. O.; Vistad, Ø. B.; Knudsen, K. D.; Roots, J.; Pedersen, J. S.; Norby, P. *J. Mater. Chem.* **2007**, *17*, 965. (b) Johnsen, R. E.; Norby, P. *J. Appl. Crystallogr.* **2008**, *41*, 991. (c) Johnsen, R. E.; Wu, Q.-L.; Sjåstad, A. O.; Vistad, Ø. B.; Krumeich, F.; Norby, P. *J. Phys. Chem. C* **2008**, *112*, 16733. (d) Hansen, E. W.; Norby, P.; Roots, J.; Wu, Q.-L. *J. Phys. Chem. C* **2007**, *111*, 11854.
(16) (a) Furubayashi, Y.; Hitosugi, T.; Yamamoto, Y.; Inaba, K.; Kinoda, G.; Hirose, Y.; Shimada, T.; Hasegawa, T. *Appl. Phys. Lett.* **2005**, *86*, 252101. (b) Wan, Q.; Wang, T.-H. *Appl. Phys. Lett.* **2006**, *88*, 226102. (c) Furubayashi, Y.; Hitosugi, T.; Hasegawa, T. *Appl. Phys. Lett.* **2006**, *88*, 226103.
(17) Hitosugi, T.; Furubayashi, Y.; Ueda, A.; Itabashi, K.; Inaba, K.; Hirose, Y.; Kinoda, G.; Yamamoto, Y.; Shimada, T.; Hasegawa, T. *Jpn. J. Appl. Phys.* **2005**, *44*, L1063.

Published on Web 06/17/2009

To obtain substituted-titanate nanosheets, the most critical step is to produce single-phase substituted layered titanates with strict control on the substitution level and a homogeneous distribution of the substituent on the Ti sites. Previously, layered titanates with Ti sites partially substituted with lower valent cations, for example, Mg,[18] Fe, and Ni[19] were successfully synthesized by solid state reactions, whereas synthesis of layered titanates substituted with higher valent cations as Nb and Ta by solid state reaction is difficult, and a long reaction time as well as high temperature (at least 1500 °C) is required to obtain single-phase samples.[20] In general, sol−gel methods are often capable of providing samples that are homogeneous and fully reacted at much lower temperatures than by solid-state synthesis. However, it is reported that it is difficult to obtain stable precursor gels of titanates because of the high ion concentration.[21] On the basis of the above motivation, we have therefore developed a novel synthesis route, sol−gel assisted solid-state reaction (SASSR), for preparing single-phase layered Nb-substituted titanates ($Na_2Ti_{3-x}Nb_xO_7$ and $Cs_{0.7}Ti_{1.8-x}Nb_xO_4$). The produced single-phase materials are planned to be used as precursors for thin film formation. The obtained products were characterized by means of X-ray powder diffraction (XRD), scanning electron microscopy (SEM), inductively coupled plasma-atomic emission spectrometry (ICP-AES), Raman spectroscopy, and thermogravimetric analysis (TGA). Considering that the proton-exchange process and the interlayer environment of the layered titanates greatly affect the swelling and subsequent exfoliation properties,[22] the effects of Nb on the proton-exchange properties of the two titanates were also studied in the present work.

2. Experimental Section

2.1. Reagents and Materials. Titanium isopropoxide [$Ti(OC_3H_7)_4$, 97%], niobium ethoxide [$Nb(OC_2H_5)_5$, 99.95%], sodium carbonate (Na_2CO_3, 99.9%), cesium carbonate (Ce_2CO_3, 99.9%), anatase nanopowder (TiO_2, 99.7%, < 25 nm), niobium oxide (Nb_2O_5, 99.99%), ammonium carbonate [$(NH_4)_2CO_3$, 99.0%], sodium acetate (CH_3COONa, 99.0%), and cesium acetate (CH_3COOCe, 99.0%) were purchased from Sigma-Aldrich Co. and used as received. Isopropanol [$CH_3CH(OH)CH_3$], nitric acid (HNO_3), and hydrochloric acid (HCl) were purchased from Fluka Chemical Co. with analytical grade purity.

2.2. Synthesis of Nb-Substituted Titanates by SASSR. The SASSR synthesis of layered titanates consists of two separate steps; first, a reactive nanopowder of doped titanium dioxide is prepared. Thereafter, the doped titanium dioxide powder is reacted together with alkali carbonates by a solid-state reaction to form the substituted layered titanates.

The Nb-substituted TiO_2 nanoparticles were prepared through a sol−gel procedure similar to that reported in the literature.[23] The precursors [$Ti(OC_3H_7)_4$ and $Nb(OC_2H_5)_5$] were dissolved in isopropanol with the target concentrations for substitution. A transparent sol was formed by adding the solution to weak nitric acid (0.1 M) under stirring conditions. The final composition of the constituents was set to satisfy $Ti/HNO_3/H_2O = 1:1:100$ in molar ratio. Gelation of the sol was achieved by increasing pH to 9 using an aqueous solution of ammonium carbonate (1 M). The gel was freeze-dried and then calcined at 500 °C for 2 h in air to obtain $Ti_{1-\alpha}Nb_\alpha O_2$ powders, which were used as precursors for $Na_2Ti_{3-x}Nb_xO_7$ ($\alpha = x/3$) and $Cs_{0.7}Ti_{1.8-x}Nb_xO_4$ ($\alpha = x/1.8$), respectively. X-ray powder diffraction proved the materials to be single phase anatase.

Nb-substituted titanates of $Na_2Ti_{3-x}Nb_xO_7$ ($x = 0.01-0.09$) and $Cs_{0.7}Ti_{1.8-x}Nb_xO_4$ ($x = 0.01-0.06$) were prepared by calcining a mixture of $Ti_{1-\alpha}Nb_\alpha O_2$ and Na_2CO_3 ($\alpha = x/3$) or Cs_2CO_3 ($\alpha = x/1.8$) in a molar ratio of 1.1:3 or 1:5.3, respectively, at 800 °C for 1 h to eliminate CO_2. Thereafter, the mixtures were reground and reheated twice at 800 °C in air for 20 h.

2.3. Synthesis of Nb-Substituted Titanates by Conventional Solid State Reaction. By applying a standard solid state reaction, $Na_2Ti_{3-x}Nb_xO_7$ ($x = 0.01-0.09$) was synthesized by first calcining a mixture of Na_2CO_3, TiO_2, and Nb_2O_5 in the proper molar ratio at 800 °C for 1 h to eliminate CO_2. Then the mixture was reground and reheated twice at 800−1200 °C in air for 20 h. $Cs_{0.7}Ti_{1.8-x}Nb_xO_4$ ($x = 0.01-0.06$) was synthesized by reacting Cs_2CO_3, TiO_2, and Nb_2O_5 in the proper molar ratio under the same heat treatment as for $Na_2Ti_{3-x}Nb_xO_7$.

2.4. Synthesis of Nb-Substituted Titanates by Conventional Sol−Gel Process. Using the sol−gel route,[11] the samples were synthesized as follows: titanium isopropoxide and niobium ethoxide (the same chemicals as the above) with a prefixed molar ratio were dissolved in isopropanol, and was then introduced dropwise into an aqueous solution of sodium acetate (or cesium acetate) under stirring. The pH of the mixture was adjusted to 4 by adding nitric acid (1 M) dropwise to obtain a transparent sol. Gelification of the sol was achieved by heating at 60 °C for 24 h. Finally the gel was calcined at 800 °C in air for 2−12 h.

2.5. Proton-Exchange of Alkali Nb-Substituted Titanates. The proton-exchanged forms of the Nb-substituted titanates were obtained by suspending 1.0 g sample in 1 M HCl (100 mL) for 3 days, refreshing the acid solution every day. The solid products were filtered, rinsed with water, and dried in air at room temperature.

2.6. Characterization. The formed materials were characterized by XRD (Siemens D5000 powder diffractometer in Bragg−Brentano geometry and with Cu $K\alpha_1$ radiation), SEM (FEI Quanta 200 F, operated at an accelerating voltage of 30 kV), and TGA (Perkin-Elmer TGA 7 system; N_2 flow, heating rate: 10 °C/min). The composition of the materials was determined by ICP-AES (Vista Ax. CCD Simultaneous ICP-AES). Raman scattering spectra of the as-prepared samples were recorded with a spectrometer from Horiba (Jobin Yvon) model T64000 at room temperature. The samples were illuminated with a 632.8 nm He−Ne laser on an Olympus BX 40 confocal microscope with a 50× objective. A laser power (1 mW) and an exposure time of 30 s was used. The resolution of the Raman spectra at room temperature is about 2 cm^{-1}.

3. Results and Discussion

3.1. Structural Properties and Morphology. The as-synthesized layered titanates were investigated by means of X-ray powder diffraction to evaluate the completion of the reaction and phase purity. XRD patterns of the samples prepared by the SASSR route with different amounts of Nb are presented in Figure 1, and the identified phases are listed in Table 1. For $x < 0.09$ the Nb-substituted sodium tri-titanates ($Na_2Ti_{3-x}Nb_xO_7$) were concluded to be phase pure, showing only reflections corresponding to a $Na_2Ti_3O_7$-like phase (Figure 1a). All

(18) (a) Machida, M.; Ma, X.-W.; Taniguchi, H.; Yabunaka, J.; Kijima, T. *J. Mol. Catal. A: Chem.* **2000**, *155*, 131. (b) Gao, T.; Fjellvåg, H.; Norby, P. *J. Mater. Chem.* **2009**, *19*, 787.
(19) Harada, M.; Sasaki, T.; Ebina, Y.; Watanabe, M. *J. Photochem. Photobiol., A* **2000**, *148*, 273.
(20) Maso′, N.; Beltra′, H.; Cordoncillo, E.; Sinclair, D. C.; West, A. R. *J. Am. Ceram. Soc.* **2008**, *91*, 144.
(21) Baliteau, S.; Sauvet, A. L.; Lopez, C.; Fabry, P. *Solid State Ionics* **2007**, *178*, 1517.
(22) Sasaki, T.; Watanabe, M.; Michiue, Y.; Komatsu, Y.; Izumi, F.; Takenouchi, S. *Chem. Mater.* **1995**, *7*, 1001.
(23) Sotter, E.; Vilanova, X.; Llobet, E.; Stankova, M.; Correig, X. *J. Optoelectron. Adv. Mater.* **2005**, *7*, 1395.

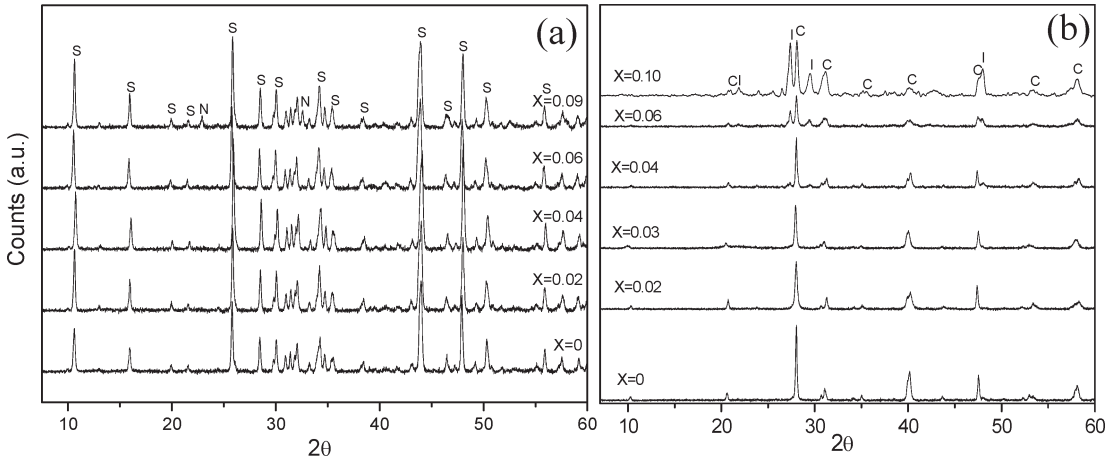

Figure 1. XRD patterns of (a) $Na_2Ti_{3-x}Nb_xO_7$ and (b) $Cs_{0.7}Ti_{1.8-x}Nb_xO_4$ synthesized by the SASSR route (S = $Na_2Ti_3O_7$-like phase, N = $NaNbO_3$, C = $Cs_{0.7}Ti_{1.8}O_4$-like phase; I = $Cs_2Ti_4O_9$).

Table 1. Evaluation of Titanates Phases Detected by XRD

compound formulas	synthesis method	Nb content (x)	phases detected by XRD
$Na_2Ti_{3-x}Nb_xO_7$	solid-state reaction	0	$Na_2Ti_3O_7$
		0.03	$Na_2Ti_3O_7$* and $NaNbO_3$
		0.06	$Na_2Ti_3O_7$* and $NaNbO_3$
	sol−gel	0	$Na_2Ti_3O_7$ and $Na_2Ti_6O_{13}$
		0.03	$Na_2Ti_3O_7$* and $Na_2Ti_6O_{13}$
	SASSR	0	$Na_2Ti_3O_7$
		0.02	$Na_2Ti_3O_7$*
		0.03	$Na_2Ti_3O_7$*
		0.04	$Na_2Ti_3O_7$*
		0.06	$Na_2Ti_3O_7$*
		0.09	$Na_2Ti_3O_7$* and $NaNbO_3$
$Cs_{0.7}Ti_{1.8-x}Nb_xO_4$	solid-state reaction	0	$Cs_{0.7}Ti_{1.8}O_4$
		0.02	$Cs_{0.7}Ti_{1.8}O_4$* and unknown phase
	sol−gel	0	$Cs_{0.7}Ti_{1.8}O_4$ and anatase
		0.02	$Cs_{0.7}Ti_{1.8}O_4$* and anatase
	SASSR	0	$Cs_{0.7}Ti_{1.8}O_4$*
		0.02	$Cs_{0.7}Ti_{1.8}O_4$*
		0.03	$Cs_{0.7}Ti_{1.8}O_4$*
		0.04	$Cs_{0.7}Ti_{1.8}O_4$* and trace $Cs_2Ti_4O_9$
		0.06	$Cs_{0.7}Ti_{1.8}O_4$* and $Cs_2Ti_4O_9$
		0.10	$Cs_{0.7}Ti_{1.8}O_4$* and $Cs_2Ti_4O_9$

* Phases may include Nb.

peaks were indexed based on the monoclinic unit cell (JCPDS No.72-0148). When increasing the amount of Nb up to $x = 0.09$, peaks corresponding to $NaNbO_3$ (JCPDS No. 73-0803) appeared. For $Cs_{0.7}Ti_{1.8-x}Nb_xO_4$, single phases were obtained when $x \leq 0.03$ (Figure 1b) and all peaks were indexed according to the orthorhombic unit cell (JCPDS No.84-1226). A second phase of $Cs_2Ti_4O_9$ (JCPDS No. 32-0268) appeared for $x \geq 0.04$, but no indications of other impurity phases, such as $CsNbO_3$ were observed. With increasing amount of Nb added, the peak intensity of $Cs_2Ti_4O_9$ increased.

The similarity of the ionic radii of Nb(V) and Ti(IV) suggests that the solubility of Nb in titanate phases will depend mainly on the charge compensation mechanism rather than on the induced stress in the lattice.[24] Thus, the effect of introducing Nb is given by the following charge equilibrated equations, expressed in classical Kröger−Vink notation:

$$Nb_{Nb} + Ti_{Ti}^{x} \rightarrow Nb_{Ti}^{\bullet} + \frac{1}{4}V'''_{Ti} \quad (1)$$

$$Nb_{Nb} + Ti_{Ti}^{x} \rightarrow Nb_{Ti}^{\bullet} + T'_{Ti} \quad (2)$$

Charge compensation of Nb(V) is achieved either by the creation of one Ti vacancy per four Nb substituted or by the reduction of one Ti(IV) to Ti(III) per Nb introduced. Both mechanisms may be present, the latter being much more likely to occur at high temperatures. However, for a complete description of possible defects in Nb-substituted titanates, the occurrence of oxygen vacancies also has to be considered. It would be expected that the introduction of Nb would reduce the amount of oxygen vacancies because of the higher positive charge. [Note on notation: In all chemical compositions we have introduced Nb in the formula without changing the oxygen stoichiometry. As Nb enters the structure with a valence of V, the oxygen content should correspondingly increase if this is a regular substitution. Writing correct formulas would be very complex, and would require detailed information about, for example, defect chemistry, cation stoichiometry, and vacancy distribution. Thus we have chosen to use a simplified notation for the chemical composition. In the lepidocrocite type titanate, vacancies are present on the octahedral sites in the layer, for example, $Cs_{0.7}Ti_{1.825}\Lambda_{0.175}O_4$. We have also here used a simpler notation, for example, $Cs_{0.7}Ti_{1.8-x}Nb_xO_4$, where the vacancies are not explicitly stated.]

In Figure 2 the lattice parameters of the sodium and cesium titanates are plotted as a function of Nb substitution (x). For $Na_2Ti_{3-x}Nb_xO_7$ the unit cell volume increases almost linearly with increasing Nb content. The ionic radius of Nb(V) (0.64 Å) is larger than that of Ti(IV) (0.605 Å),[25] and the observed correlation between the

(24) Arbiol, J.; Cerdà, J.; Dezanneau, G.; Cirera, A.; Peiró, F.; Cornet, A.; Morante, J. R. *J. Appl. Phys.* **2002**, *92*, 853.

(25) Greenwood, N. N.; Earnshaw, A. *Chemistry of the Elements*, 2nd ed.; Elsevier: New York, 1998.

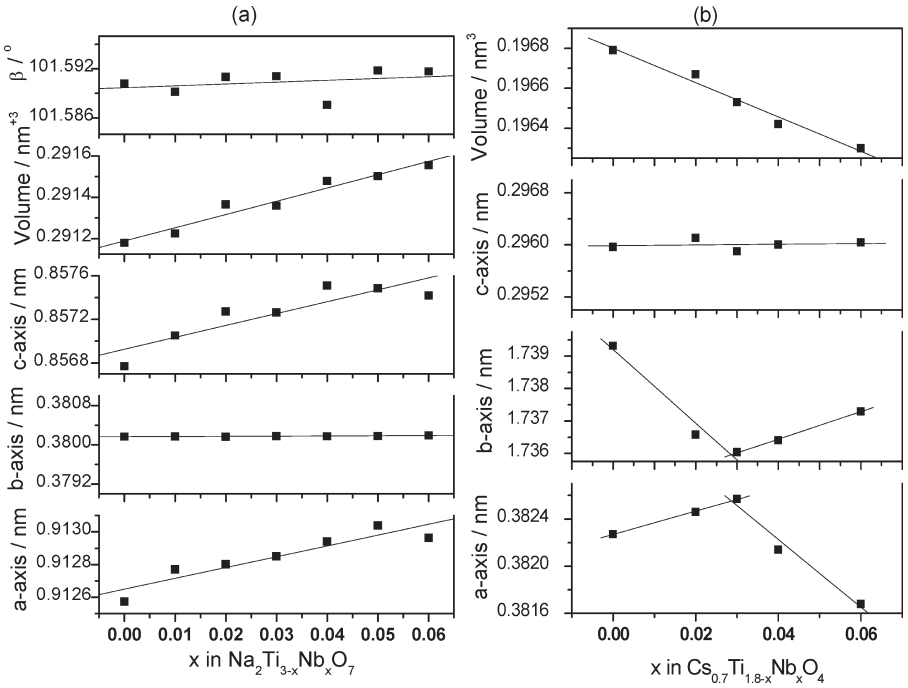

Figure 2. Unit cell parameters as a function of Nb substitution (x) for (a) $Na_2Ti_{3-x}Nb_xO_7$ and (b) $Cs_{0.7}Ti_{1.8-x}Nb_xO_4$. (The error bars are not marked in the plots because the data used are from Rietveld refinement, and the esd's are underestimated. They would be smaller than the markers.).

amount of Nb in the synthesis and the unit cell parameters indicate that Vegard's law is obeyed[26] and that Nb is incorporated in the Ti lattice as a solid solution. The increase in the unit cell volume with Nb content matches well with the niobium substituted anatase TiO_2.[27]

A more complex behavior of the unit cell volume as a function of niobium substitution is found for the lepidocrocite-type material. As seen in Figure 2b, the volume decreases as a function of niobium substitution. The *a*-axis increases between x=0−0.03, and then decreases with increasing x. The opposite trend is observed for the *b*-axis, where a decrease is observed up to $x = 0.03$, and an increase for higher niobium concentrations. The *c*-axis is almost unaffected by the niobium content. The resulting negative volume expansion with niobium substitution is probably a result of the complex defect structure of the lepidocrocite layers. From Figure 1b it appears that another titanate phase ($Cs_2Ti_4O_9$) appears when x is close to 0.03. This does not necessarily indicate a solubility limit of Nb, as the phase formed is titanate but not niobate. The decrease in volume with the increase of Nb substitution level indicates that Nb is still incorporated into the lattice for $x > 0.03$. At $x \approx 0.03$, the behavior of the *a* and *b* axes changes, which may be ascribed as follows: when $x > 0.03$, Nb enters into the lepidocrocite or $Cs_2Ti_4O_9$ lattice rather than separating from the titanate phase, as we observed for $Na_2Ti_{3-x}Nb_xO_7$ ($x > 0.06$). In the parent material there are approximately 9% vacancies on octahedral positions in the host layer. The defect situation after substituting titanium with niobium is unknown. The extra charges generated by Nb substitution could be compensated, for example, by additional vacancies or a decrease in the amount of alkali counterions. In addition, this is a layered structure with the layers stacked along the *b*-axis. All of this makes it difficult to predict the behavior of the unit cell parameters as a function of niobium substitution. However, the observation of systematic changes in the unit cell volume, indicate that niobium is incorporated in the material.

Figure 3 shows the XRD patterns of $Na_2Ti_{3-x}Nb_xO_7$ ($x = 0.03$) synthesized by solid state reaction at temperatures from 900 to 1200 °C. It is well-known[28] that undoped single-phase layered titanates can easily be obtained by solid state reaction at 800−900 °C. In the present work we have experienced that it is much more difficult to obtain single-phase Nb-substituted titanates than the undoped analogues by solid state reaction. From the XRD patterns presented in Figure 3 it can be observed that the amount of the impurity phase $NaNbO_3$ decreased with increasing reaction temperature. When applying a reaction temperature of 1100 °C, the $NaNbO_3$ phase disappeared but the $Na_2Ti_3O_7$-like phase started to convert into $Na_2Ti_6O_{13}$ (JCPDS No.73-1398). At 1200 °C, the alumina crucible used in the reaction reacted with the sample, and Al-doped sodium titanate was formed. We have also tried to obtain single-phase Nb-substituted titanate at relatively lower temperature (900 °C) by using much longer reaction time (the results is shown in the Supporting Information, Figure 1), but the impurity phase $NaNbO_3$ can still be observed even after prolonged annealing for 80 h. For Nb-substituted cesium titanate synthesized by solid state reaction, an unknown phase in addition to $Cs_{0.7}Ti_{1.8-x}Nb_xO_4$ is clearly observed even when small amounts of Nb_2O_5 ($x = 0.02$) were added (the XRD pattern is shown in the Supporting Information, Figure 2).

(26) Denton, A. R.; Ashcroft, N. W. *Phys. Rev. A* **1991**, *43*, 3161.
(27) Sacerdoti, M.; Dalconi, M. C.; Carotta, M. C.; Cavicchi, B.; Ferroni, M.; Colonna, S.; Vona, M. L. *J. Solid State Chem.* **2004**, *177*, 1781.
(28) Sasaki, T. *J. Ceram. Soc. Jpn.* **2007**, *115*, 9.

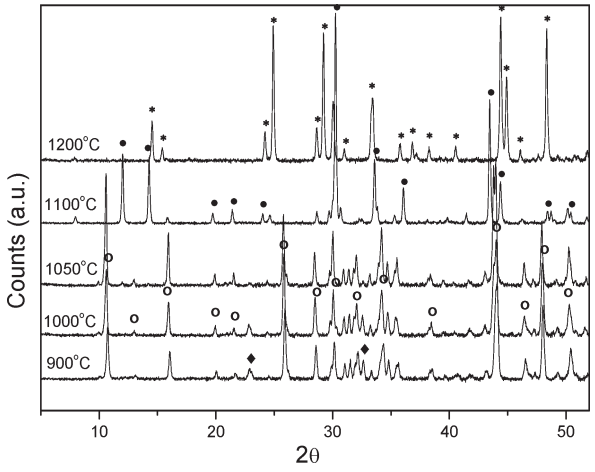

Figure 3. XRD patterns of $Na_2Ti_{3-x}Nb_xO_7$ ($x = 0.03$) synthesized by solid state reaction at selected temperatures between 900 and 1200 °C. (○: $Na_2Ti_3O_7$-like phase; ●: $Na_2Ti_6O_{13}$-like phase; ♦: $NaNbO_3$, and *: $Na_{1.97}Al_{1.82}Ti_{6.15}O_{16}$).

Table 2. ICP-AES Results of $Na_2Ti_{3-x}Nb_xO_7$ and $Cs_{0.7}Ti_{1.8-x}Nb_xO_4$

samples	nominal ratios (A/Ti/Nb)[a]	Real ratios determined by ICP-AES (A/Ti/Nb)[a]
$Na_2Ti_{3-x}Nb_xO_7$		
$x = 0.03$	1/1.485/0.015	1/1.49/0.015
$x = 0.06$	1/1.47/0.03	1/1.47/0.032
$Cs_{0.7}Ti_{1.8-x}Nb_xO_4$		
$x = 0.02$	0.70/1.805/0.02	0.77/1.98/0.02
$x = 0.03$	0.70/1.795/0.03	0.70/1.8/0.032

[a] A = Na or Cs.

The conventional sol−gel route was also attempted to obtain homogeneously Nb-substituted sodium and cesium titanates. As seen from the XRD results reported in Table 1 (the XRD patterns are shown in the Supporting Information, Figures 3 and 4), impurity phases are observed for both $Na_2Ti_3O_7$ and $Cs_{0.7}Ti_{1.8}O_4$ even without adding Nb, and the content of the impurity phases increased with increasing calcination temperature or when prolonging the calcination time. In addition, the impurity phase $NaNbO_3$ is also clearly observed in $Na_2Ti_{3-x}Nb_xO_7$ for $x = 0.03$.

For synthesis of single-phase Nb-substituted titanates, the XRD clearly reveal that the SASSR synthesis route is superior to both the solid state reaction and the sol−gel route. Real compositions of the two kinds of materials were determined by ICP-AES, and the results listed in Table 2 are consistent with the nominal values. In the following, characterization by means of SEM and Raman spectroscopy of the single-phase products obtained by the SASSR route is further discussed.

The morphology of sodium and cesium titanates substituted with different Nb amount were examined by SEM (Figure 4). The as-synthesized $Na_2Ti_{3-x}Nb_xO_7$ samples (Figure 4, panels a, b, and c) show an interpenetrating aggregation of polygonal crystals with length of several micrometers and a thickness of around 500 nm. There is no notable difference between the morphology of the $Na_2Ti_{3-x}Nb_xO_7$ microcrystals without ($x = 0$, Figure 4a) and with Nb substitution ($x = 0.03$ and 0.06, Figure 4, panels b and c). The as-prepared $Cs_{0.7}Ti_{1.8-x}Nb_xO_4$ ($x = 0$, Figure 4d) is a microcrystalline powder of micrometer dimension with plate-like morphology. With increasing Nb content, the lengths of the grains increased and the majority of the grains appeared more rod-shaped as shown in Figure 4 panels e and f. The crystal surfaces of the samples are clean and smooth, revealing that no Nb phases are separated out from the substituted titanate structure, supporting formation of pure phases where Nb is incorporated in the Ti lattice as a solid solution.

The Raman spectra of $Na_2Ti_{3-x}Nb_xO_7$ are presented in Figure 5a. The set of observed bands and spectrum features agrees well with the reported Raman data for $Na_2Ti_3O_7$.[29,30] The bands at about 290 and 307 cm^{-1} are ascribed to the Na−Ti−O stretching vibration,[29] and the bands in the high-wavenumber region (500−1000 cm^{-1}) originated from the Ti−O−Ti stretching vibrations.[30] All spectra are almost identical independent of the degree of Nb substitution. The Ti-site located at the center of an oxygen octahedron is a highly symmetric point when the octahedron is not distorted. The similarity in the Raman spectra with increasing Nb content suggest that the substitutional effect of Nb at the Ti site in sodium titanate is minor. No other bands appear when Nb is introduced into the TiO_6 lattice, indicating that the as-prepared $Na_2Ti_{3-x}Nb_xO_7$ ($x \leq 0.06$) samples are single phase, which is also consist with the XRD patterns (Figure 1a).

The Raman spectra of $Cs_{0.7}Ti_{1.8-x}Nb_xO_4$ are shown in Figure 6a. The bands in the region of 100−900 cm^{-1} can be ascribed to the stretching vibration of Ti−O−Ti bonds in the host layer. There is no significant difference in the Raman spectra between the samples with $x = 0$ and $x = 0.02$, while the bands around 440 and 640 cm^{-1}, corresponds to the Ti−O bending and stretching vibration involving six-coordinated oxygen,[31] shift toward higher wavenumber at higher Nb substitution level. This suggests that the octahedron in the host layer is distorted when the amount of Nb is increased to $x = 0.03$. At the same time, the intensities of the bands at 850−950 cm^{-1} also changed when substituted with Nb. Kudo et al.[32] reported the Raman spectra of a lepidocrocite-type titanate ($Cs_2Ti_6O_{13}$). They assigned the bands at 850−950 cm^{-1} to the stretching modes of Ti−O bonds that stick out into the interlayer space. Thus, the changes of the intensities of the bands at 850−950 cm^{-1} suggest that the force constant of the Ti−O bonds that stick out into the interlayer space change,[33] which is consistent with the change in unit cell parameters in Figure 2b, where the *b*-axis changes significantly more than the *a* and *c*-axes with increasing Nb substitution. This effect is also confirmed by the ion-exchange properties of cesium titanate that will be discussed in the next section.

3.2. Properties of Proton-Exchanged Samples. Raman spectra of proton-exchanged samples of $H_2Ti_{3-x}Nb_xO_7$ and $H_{0.7}Ti_{1.8-x}Nb_xO_4 \cdot nH_2O$ are presented in Figure 5b

(29) Papp, S.; Kõrösi, L.; Meynen, V.; Cool, P.; Vansant, E. F.; Dékány, I. *J. Solid State Chem.* **2005**, *178*, 1614.
(30) Bamnerger, C.; Begun, G. *J. Am. Ceram. Soc.* **1987**, *70*, C-48.
(31) Ma, R. Zh.; Fukuda, K.; Sasaki, T.; Osada, M.; Bando, Y. *J. Phys. Chem. B* **2005**, *109*, 6210.
(32) Kudo, A.; Kondo, T. *J. Mater. Chem.* **1997**, *7*, 777.
(33) Hushur, A.; Ko, J.-H.; Kojima, S. *J. Korean Phys. Soc.* **2002**, *41*, 763.

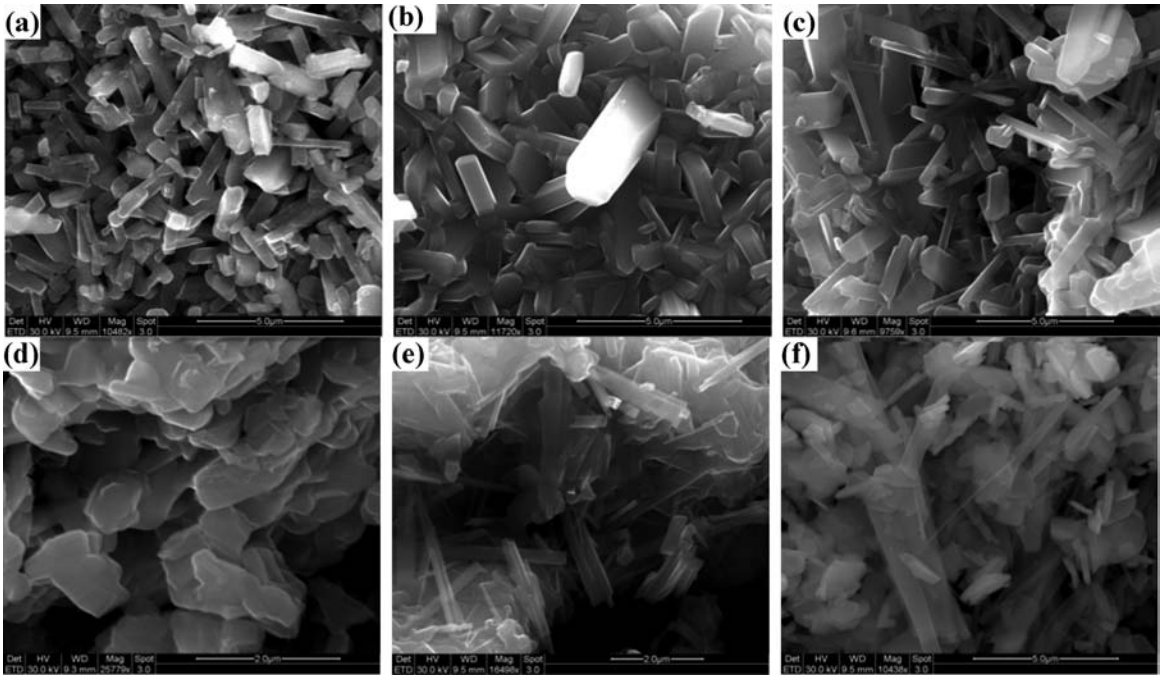

Figure 4. SEM images of $Na_2Ti_{3-x}Nb_xO_7$, (a) $x = 0$, (b) $x = 0.03$, (c) $x = 0.06$ and $Ce_{0.7}Ti_{1.8-x}Nb_xO_4$, (d) $x = 0$, (e) $x = 0.02$, (f) $x = 0.03$.

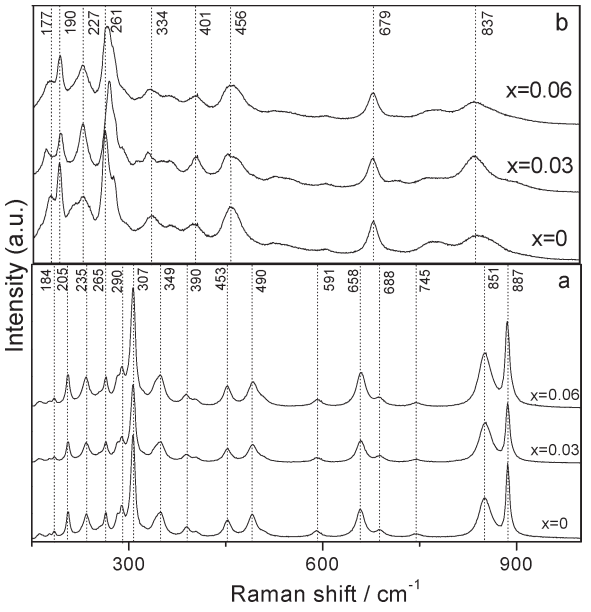

Figure 5. Raman spectra of (a) $Na_2Ti_{3-x}Nb_xO_7$ and (b) its proton-exchanged form.

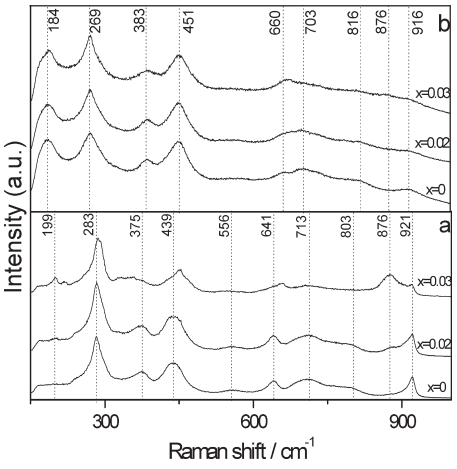

Figure 6. Raman spectra of (a) $Cs_{0.7}Ti_{1.8-x}Nb_xO_4$ and (b) its proton-exchanged form.

and Figure 6b, respectively. In Figure 5b, the bands assigned to the Na−Ti−O stretching vibrations (~290 and 307 cm^{-1}) and the stretching vibration of short Ti−O bonds involving nonbridging oxygen coordinated with sodium ion (~887 cm^{-1}) were not observed after the ion exchange process, indicating that there are no sodium ions in the proton-exchanged samples. In Figure 6b the band contributed to Cs−O stretching vibration (~921 cm^{-1}) can also hardly be observed in the proton-exchanged cesium titanate. It is interesting to observe from the Raman spectra that the distortion of the octahedron in the lepidocrocite-type structure disappeared after proton-exchange.

Figure 7 shows the XRD patterns of the proton-exchanged products. The patterns of $H_2Ti_{3-x}Nb_xO_7$ (Figure 7a) are in agreement with literature,[34] and there is no difference between samples doped with different amounts of Nb. However, in the patterns of $H_{0.7}Ti_{1.8-x}Nb_xO_4 \cdot nH_2O$ (Figure 7b, c), a highly swollen phase ($d = 1.05$ nm) is observed when doped with Nb, and the intensity of the peak related to the swollen phase increased by increasing Nb content.

The lattice parameters of the proton-exchanged samples are summarized in Table 3. It can be observed that the *a*-axis increases with the degree of proton-exchange of $Na_2Ti_{3-x}Nb_xO_7$. However, a simultaneous small decrease in the *b*-axis reflects a contraction in the interlayer distance probably because of the exchange of Na^+ for H^+

(34) Miyamoto, N.; Kurodaa, K.; Ogawa, M. *J. Mater. Chem.* **2004**, *14*, 165.

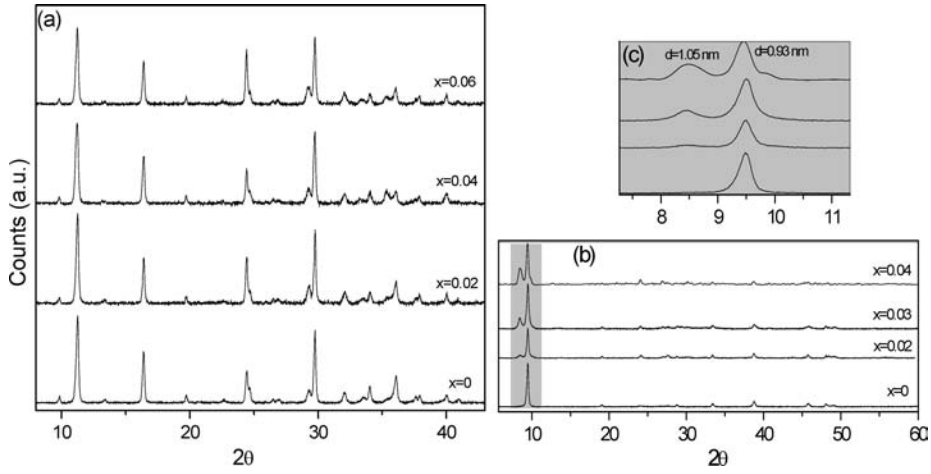

Figure 7. XRD patterns of proton-exchanged titanates; (a) $H_2Ti_{3-x}Nb_xO_7$; (b) $H_{0.7}Ti_{1.8-x}Nb_xO_4 \cdot H_2O$; and (c) enlarged patterns of the gray section in (b).

Table 3. Unit Cell Parameters of the Proton-Exchanged Titanates Samples

samples		lattice parameters[a]				
titanates	content of Nb (x)	a (nm)	b (nm)	c (nm)	Beta (°)	Vol (nm^3)
$H_2Ti_{3-x}Nb_xO_7$	0	1.6168(1)	0.3749(2)	0.9202(6)	101.77(1)	0.5461(1)
	0.03	1.6379(1)	0.3746(3)	0.9246(6)	102.41(1)	0.5541(1)
	0.06	1.6238(2)	0.3750(2)	0.9222(6)	102.07(1)	0.5491(1)
$H_{0.7}Ti_{1.8-x}Nb_xO_4 \cdot nH_2O$	0	0.3774(9)	1.8559(7)	0.2968(6)		0.2079(1)
	0.02	0.3760(6)	1.8572(3)	0.2973(3)		0.2076(1)
	0.03	0.3767(1)	1.8573(9)	0.2973(9)		0.2080(1)
	0.04	0.3767(2)	1.8652(3)	0.2990(9)		0.2101(1)

[a] The data in the bracket are the esd's from refinement.

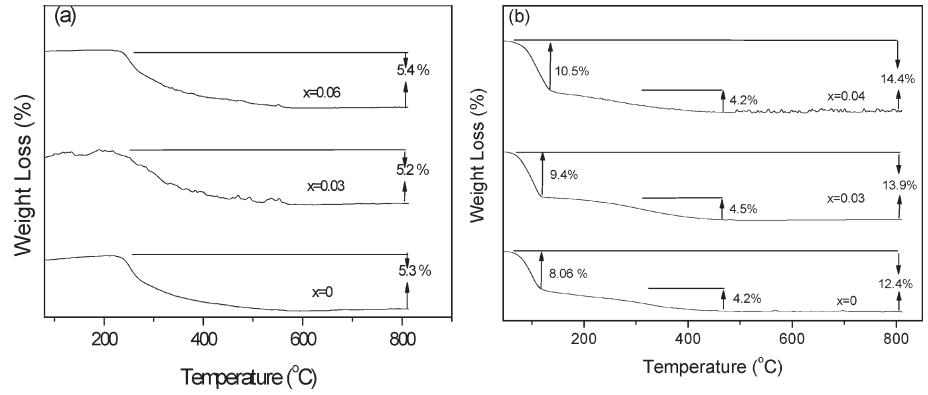

Figure 8. TG of proton-exchanged titanates; (a) $H_2Ti_{3-x}Nb_xO_7$ and (b) $H_{0.7}Ti_{1.8-x}Nb_xO_4 \cdot H_2O$.

without change in the host Ti_3O_7 layers.[22] No weight loss could be observed by TGA (Figure 8a) below 240 °C, showing that the proton-exchanged compounds $H_2Ti_{3-x}Nb_xO_7$ do not contain interlayer water.

For the orthorhombic $Cs_{0.7}Ti_{1.8-x}Nb_xO_4$ phase, the b-axis increased whereas the a- and c-axes changed only slightly after proton-exchange, indicating an expansion of the interlayer distance without changes in the host layer. In contrast to $H_2Ti_{3-x}Nb_xO_7$, the interlayer distance of $H_{0.7}Ti_{1.8-x}Nb_xO_4 \cdot nH_2O$ increased slightly with increasing Nb content, suggesting that the Nb added may enlarge the interlayer space of $H_{0.7}Ti_{1.8-x}Nb_xO_4 \cdot nH_2O$. This is significant for the subsequent exfoliation of the layered structure into a single layer because the interlayer interactions are important for the intercalation and delamination behavior of the protonic layered titanates.[22] These results were also confirmed by TGA (Figure 8b). The interlayer water molecules of $H_{0.7}Ti_{1.8-x}Nb_xO_4 \cdot nH_2O$ calculated from the TGA results are approximately 0.74 mol ($x = 0$), 0.88 mol ($x = 0.03$), and 0.99 mol ($x = 0.04$) per formula weight, respectively, which implies that more water molecules were intercalated into the interlayer of $H_{0.7}Ti_{1.8-x}Nb_xO_4 \cdot nH_2O$ with increasing Nb-substitution.

4. Conclusions

In summary, single-phase layered Nb-substituted titanates, $Na_2Ti_{3-x}Nb_xO_7$ ($x = 0-0.06$) and $Cs_{0.7}Ti_{1.8-x}Nb_xO_4$ ($x = 0-0.03$), were successfully synthesized by a new sol−gel

assisted solid state reaction (SASSR) route. The conventional sol−gel and solid state reactions failed to give single-phase Nb-substituted titanate materials. In the SASSR route we combine the advantages of the sol−gel and solid state reaction techniques. The results reported here clearly reveal that Ti(IV) in the host layer can be partially substituted by Nb(V) without structural deterioration. After proton-exchange, the number of water molecules in the interlayer region of $H_{0.7}Ti_{1.8-x}Nb_xO_4 \cdot nH_2O$ increased with increasing degree of niobium substitution, which is beneficial for the subsequent exfoliation process. On the contrary, the interlayer distances in $H_2Ti_{3-x}Nb_xO_7$ ($x = 0-0.06$) are only slightly dependent on the niobium substitution.

Ongoing work has shown that the SASSR route can also be applied for the synthesis of titanates substituted by other ions with higher valent, such as Ta and W. Furthermore, it is expected that the SASSR route could also be applied to other kinds of titanates.

Acknowledgment. We thank Professor C. J. Nielsen and Dr. Anna Magrasó for their help on the Raman and SEM measurements, respectively. We also thank Dr. Ruikai Xie for his help on the ICP-AES measurement. The authors acknowledge the financial assistance from the Research Council of Norway (NANOMAT, Grant 163565 431 Pr Chem).

Supporting Information Available: Additional information as noted in the text. This material is available free of charge via the Internet at http://pubs.acs.org.